

Halo clustering and g_{NL} -type primordial non-Gaussianity

Kendrick M. Smith¹, Simone Ferraro¹, and Marilena LoVerde²

¹ *Princeton University Observatory, Peyton Hall, Ivy Lane, Princeton, NJ 08544 USA*

² *Institute for Advanced Study, Einstein Drive, Princeton, NJ 08540, USA*

Abstract

A wide range of multifield inflationary models generate non-Gaussian initial conditions in which the initial adiabatic fluctuation is of the form $(\zeta_G + g_{NL}\zeta_G^3)$. We study halo clustering in these models using two different analytic methods: the peak-background split framework, and brute force calculation in a barrier crossing model, obtaining agreement between the two. We find a simple, theoretically motivated expression for halo bias which agrees with N -body simulations and can be used to constrain g_{NL} from observations. We discuss practical caveats to constraining g_{NL} using only observable properties of a tracer population, and argue that constraints obtained from populations whose observed bias is $\lesssim 2.5$ are generally not robust to uncertainties in modeling the halo occupation distribution of the population.

1 Introduction

In the last few decades, increasingly precise observations (e.g. [1–6]) have led to a standard cosmological model in which small initial fluctuations evolve in a Λ CDM background to give rise to the observed universe. Current data are consistent with initial fluctuations which are adiabatic, scalar, Gaussian, with weak deviations from scale invariance ($n_s < 1$ at 3σ).

The statistics of the initial fluctuations, i.e. deviations from Gaussian initial conditions, provide a powerful probe of the physics of the early universe. In the context of inflation [7–13], the simplest models (single-field, minimally coupled slow-roll) predict initial curvature perturbations with negligible deviations from Gaussianity. However, there is a rich phenomenology of non-Gaussian initial conditions in models with multiple fields, self-interactions near horizon crossing, or speed of sound $c_s \ll 1$ during inflation. In this paper, we will focus on non-Gaussianity of the so-called local type [14–17], in which the primordial potential¹ is of the form

$$\Phi(\mathbf{x}) = \Phi_G(\mathbf{x}) + f_{NL}(\Phi_G(\mathbf{x})^2 - \langle \Phi_G^2 \rangle) + g_{NL}(\Phi_G(\mathbf{x})^3 - 3\langle \Phi_G^2 \rangle \Phi_G(\mathbf{x})) \quad (1)$$

where Φ_G is a Gaussian field and f_{NL} , g_{NL} are free parameters.²

Local non-Gaussianity can be generated by physical mechanisms involving multiple fields, such as light spectator fields during inflation which evolve to generate the initial adiabatic fluctuations (the curvaton scenario) [18–20], or models where the inflaton decay rate is modulated by a second field [21, 22]. Non-Gaussianity of local type is also naturally generated in non-inflationary models of the early universe such as the new ekpyrotic/cyclic scenario [23–25]. There is a theorem [26, 27] which states that any single-field model of inflation cannot generate detectable levels of local non-Gaussianity without violating observed limits on deviation from a scale-invariant power spectrum. Thus, detection of either f_{NL} or g_{NL} would rule out all single field models of inflation and place powerful constraints on the physics of the early universe. Current observational constraints on these parameters are consistent with zero [1, 28–30], but are expected to improve by an order of magnitude or more in the near future.

In models of inflation in which $|g_{NL}| = \mathcal{O}(f_{NL}^2)$, it is unlikely that observational constraints on g_{NL} will be competitive with constraints on f_{NL} . However, there are a number of examples where $f_{NL}^2 \ll |g_{NL}|$, making the g_{NL} term in Eq. (1) the dominant source of primordial non-Gaussianity. This situation arises in curvaton models where non-quadratic terms in the potential are important [31–35] or in multifield models in which (ΔN) varies rapidly at the end of inflation [36, 37]. The existence of these scenarios makes searching for g_{NL} just as important as f_{NL} and measurements provide important constraints on the microphysical parameter space.

In a pioneering paper [38], Dalal et al showed that large-scale clustering of halos depends sensitively on f_{NL} . More precisely, a sample of halos (or tracers such as galaxies or quasars) with

¹In studies of primordial non-Gaussianity, it is conventional to define a primordial potential $\Phi = \frac{3}{5}\zeta$, where ζ is the initial adiabatic curvature perturbation. Note that Φ is not the conformal Newtonian potential, which is given by $\frac{2}{3}\Phi$ deep in the radiation-dominated epoch where Eq. (1) applies.

²We define g_{NL} -type non-Gaussianity including the term $-3\langle \Phi_G^2 \rangle \Phi_G$; this term simply renormalizes Φ_G so that its power spectrum P_{Φ_G} is equal to the observed power spectrum P_Φ (to first order in g_{NL}).

constant bias b_1 in a Gaussian cosmology will have scale-dependent bias given by

$$b(k) \approx b_1 + 2\delta_c(b_1 - 1) \frac{f_{NL}}{\alpha(k, z)} \quad (2)$$

in an f_{NL} cosmology. Here, δ_c is the spherical collapse threshold and $\alpha(k, z)$ is defined by

$$\alpha(k, z) = \frac{2k^2 T(k) D(z)}{3\Omega_m H_0^2} \quad (3)$$

so that the linear density field and the primordial potential are related by $\delta_{\text{lin}}(k, z) = \alpha(k, z)\Phi(k)$. Large-scale structure constraints on f_{NL} from scale-dependent bias are currently competitive with the CMB (e.g. [28, 39]) and may ultimately provide constraints which are stronger (e.g. [40, 41]). The key identity (2) has been derived using several different analytic frameworks [28, 42, 43] and agrees with N -body simulations (e.g. [30, 38, 44, 45]).

In this paper we study the related issue of large-scale halo-clustering in a g_{NL} cosmology. We consider the large-scale halo bias in two analytic frameworks: the peak-background split (§3) and a barrier crossing model (§4). We find consistency between the two formalisms (in disagreement with [46]) and obtain an expression analogous to Eq. (2) for the scale-dependent halo bias in a g_{NL} cosmology. Our main results are a universal relation between the scale-dependent halo bias in a g_{NL} cosmology and the mass function in an f_{NL} cosmology,

$$b(k) \approx b_1 + \frac{\beta_g g_{NL}}{\alpha(k, z)} \quad \text{where} \quad \beta_g = 3(\partial \log n / \partial f_{NL}) \quad (4)$$

and expressions for β_g (Eqs. (50), (51)) which can be used in practice to constrain g_{NL} from data. We also discuss caveats when estimating the g_{NL} bias from observable quantities (§5.4) and argue that constraints obtained from tracer populations which are not highly biased ($b_1 \gtrsim 2.5$) are generally not robust to uncertainties in HOD modeling.

Throughout this paper we use the WMAP5+BAO+SN fiducial cosmology [47], with baryon density $\Omega_b h^2 = 0.0226$, CDM density $\Omega_c h^2 = 0.114$, Hubble parameter $h = 0.70$, spectral index $n_s = 0.961$, optical depth $\tau = 0.080$, and power-law initial curvature power spectrum $k^3 P_\zeta(k) / 2\pi^2 = \Delta_\zeta^2 (k/k_{\text{piv}})^{n_s - 1}$ where $\Delta_\zeta^2 = 2.42 \times 10^{-9}$ and $k_{\text{piv}} = 0.002 \text{ Mpc}^{-1}$. All power spectra and transfer functions have been computed using CAMB [48].

2 Definitions and notation

We will sometimes model halos of mass $\geq M$ with peaks in a smoothed density field δ_M defined as follows. Let $\delta_M(\mathbf{x})$ be the *linear* density field smoothed by a tophat filter with radius $R(M) = (3M/4\pi\rho_m)^{1/3}$, i.e.

$$\delta_M(\mathbf{x}) = \int \frac{d^3\mathbf{k}}{(2\pi)^3} e^{-i\mathbf{k}\cdot\mathbf{x}} \delta_{\text{lin}}(\mathbf{k}) W_M(k) \quad (5)$$

where

$$W_M(k) = 3 \frac{\sin(kR(M)) - kR(M) \cos(kR(M))}{(kR(M))^3} \quad (6)$$

Let $\sigma_M = \langle \delta_M^2 \rangle^{1/2}$ be the RMS amplitude of the smoothed density field, and let $\kappa_n(M)$ be its n -th non-Gaussian cumulant, defined by:

$$\kappa_n(M) = \frac{\langle \delta_M^n \rangle_{\text{conn}}}{\sigma_M^n}. \quad (7)$$

Since δ_M and σ_M are defined via linear theory, $\kappa_n(M)$ is independent of redshift as implied by the notation. To first order in f_{NL} and g_{NL} , we have

$$\kappa_3(M) = \kappa_3^{(1)}(M) f_{NL} \quad (8)$$

$$\kappa_4(M) = \kappa_4^{(1)}(M) g_{NL} \quad (9)$$

with higher cumulants equal to zero, where $\kappa_3^{(1)}(M), \kappa_4^{(1)}(M)$ are the values of the cumulants at $f_{NL} = 1$ and $g_{NL} = 1$ respectively. These values are given explicitly by:

$$\kappa_3^{(1)}(M) = \frac{6}{\sigma_M^3} \int \frac{d^3\mathbf{k} d^3\mathbf{k}'}{(2\pi)^6} W_M(k) W_M(k') W_M(|\mathbf{k} + \mathbf{k}'|) \frac{P_{mm}(k) P_{mm}(k') \alpha(|\mathbf{k} + \mathbf{k}'|)}{\alpha(k) \alpha(k')} \quad (10)$$

$$\begin{aligned} \kappa_4^{(1)}(M) &= \frac{24}{\sigma_M^4} \int \frac{d^3\mathbf{k} d^3\mathbf{k}' d^3\mathbf{k}''}{(2\pi)^9} W_M(k) W_M(k') W_M(k'') W_M(|\mathbf{k} + \mathbf{k}' + \mathbf{k}''|) \\ &\quad \times \frac{P_{mm}(k) P_{mm}(k') P_{mm}(k'') \alpha(|\mathbf{k} + \mathbf{k}' + \mathbf{k}''|)}{\alpha(k) \alpha(k') \alpha(k'')} \end{aligned} \quad (11)$$

where $\alpha(k)$ was defined previously in Eq. (3) and $P_{mm}(k)$ is the power spectrum of the linear density field, $\langle \delta_{\text{lin}}(\mathbf{k}) \delta_{\text{lin}}(\mathbf{k}') \rangle = (2\pi)^3 P_{mm}(k) \delta^{(3)}(\mathbf{k} + \mathbf{k}')$. For numerical calculation, the following fitting functions (from [49]) are convenient:

$$\kappa_3^{(1)}(M) = (6.6 \times 10^{-4}) \left(1 - 0.016 \log \left(\frac{M}{h^{-1} M_\odot} \right) \right) \quad (12)$$

$$\kappa_4^{(1)}(M) = (1.6 \times 10^{-7}) \left(1 - 0.021 \log \left(\frac{M}{h^{-1} M_\odot} \right) \right). \quad (13)$$

This paper is mainly concerned with calculating halo bias $b(k) = P_{mh}(k)/P_{mm}(k)$ to first order in f_{NL} and g_{NL} , so let us establish notation from the outset, by writing the large-scale bias in the general form:

$$b(k) = b_1 + b_{1f} f_{NL} + b_{1g} g_{NL} + \frac{\beta_f f_{NL} + \beta_g g_{NL}}{\alpha(k)} \quad (14)$$

where unlike Eq. (2) and Eq. (4) we have allowed for scale-independent corrections b_{1f} and b_{1g} from f_{NL} and g_{NL} primordial non-Gaussianity. Equation (14) defines the coefficients $b_1, b_{1f}, b_{1g}, \beta_f, \beta_g$. This equation assumes that the k -dependence is of the functional form (constant) + (constant)/ $\alpha(k)$, but we will derive this analytically (Eq. (35)) and show that it agrees with simulations (§5.1). In this notation, the Dalal et al formula (2) can be written as $\beta_f = 2\delta_c(b_1 - 1)$.

3 Peak-background split

The peak-background split formalism is a procedure for predicting halo clustering statistics on large scales. The basic idea is that a long-wavelength fluctuation in the initial curvature alters the

local abundance of halos in a way which is equivalent to perturbing parameters of the background cosmology, e.g. the matter density ρ_m or the amplitude Δ_Φ of the initial fluctuations. The use of this formalism to study halo bias in non-Gaussian cosmologies was pioneered in [28]; we will review this calculation of the bias in an f_{NL} cosmology (§3.1) and then perform an analogous calculation in the g_{NL} case (§3.2).

3.1 f_{NL} cosmology

In an f_{NL} cosmology, the initial conditions are given by:

$$\Phi(\mathbf{x}) = \Phi_G(\mathbf{x}) + f_{NL}(\Phi_G(\mathbf{x})^2 - \langle \Phi_G^2 \rangle) \quad (15)$$

To analyze the effect of a long-wavelength mode, let us decompose the *Gaussian* potential as a sum $\Phi_G = \Phi_l + \Phi_s$ of long-wavelength and short-wavelength contributions. The long/short-wavelength decomposition of the non-Gaussian potential Φ is then

$$\Phi(\mathbf{x}) = \underbrace{\Phi_l(\mathbf{x}) + f_{NL}(\Phi_l(\mathbf{x})^2 - \langle \Phi_l^2 \rangle)}_{\text{long}} + \underbrace{(1 + 2f_{NL}\Phi_l(\mathbf{x}))\Phi_s(\mathbf{x}) + f_{NL}(\Phi_s(\mathbf{x})^2 - \langle \Phi_s^2 \rangle)}_{\text{short}} \quad (16)$$

and contains explicit coupling between long and short wavelength modes of the Gaussian potential.

Let us consider how the term $(1 + 2f_{NL}\Phi_l(\mathbf{x}))\Phi_s(\mathbf{x})$ in Eq. (16) affects $n_l(\mathbf{x})$, the long-wavelength part of the halo number density field. In a local region where the long-wavelength potential takes some value Φ_l , the amplitude Δ_Φ of the small-scale modes is perturbed: $\Delta_\Phi \rightarrow (1 + 2f_{NL}\Phi_l)\Delta_\Phi$. This modifies the local halo abundance, in the same way that the global abundance would be modified if the cosmological parameter Δ_Φ were perturbed, i.e. we get a term in the long-wavelength halo density of the form $\Delta n(\mathbf{x}) = 2f_{NL}\Phi_l(\mathbf{x})(\partial n/\partial \log \Delta_\Phi)$. In addition, even in a Gaussian cosmology, there is a perturbation to the local halo abundance which is proportional to the long-wavelength part $\delta_l(\mathbf{x})$ of the density fluctuation, i.e. a term of the form $\Delta n(\mathbf{x}) = \delta_l(\mathbf{x})(\partial n/\partial \delta_l)$. Putting this together, the long-wavelength part of the halo density is given by:³

$$\begin{aligned} n_l(\mathbf{x}) &= \bar{n} + \frac{\partial n}{\partial \delta_l} \delta_l(\mathbf{x}) + 2f_{NL} \frac{\partial n}{\partial \log \Delta_\Phi} \Phi_l(\mathbf{x}) \\ &= \bar{n}(1 + b_1 \delta_l(\mathbf{x}) + \beta_f f_{NL} \Phi_l(\mathbf{x})) \end{aligned} \quad (17)$$

where

$$b_1 = \frac{\partial \log n}{\partial \delta_l} \quad (18)$$

$$\beta_f = 2 \frac{\partial \log n}{\partial \log \Delta_\Phi}. \quad (19)$$

³In this derivation, we have swept two terms in Eq. (15) under the rug; let us now argue that these are indeed negligible. The term $f_{NL}(\Phi_s(\mathbf{x})^2 - \langle \Phi_s^2 \rangle)$ alters the statistics of the small scale modes; this does perturb the halo abundance (by generating skewness in the density field) but the perturbation is independent of the long-wavelength fluctuation Φ_l . Therefore, this term does not contribute to the large-scale halo bias. The term $f_{NL}(\Phi_l(\mathbf{x})^2 - \langle \Phi_l^2 \rangle)$ perturbs the long-wavelength modes and decorrelates them (to order $\mathcal{O}(f_{NL})$) from both the linear density fluctuation $\delta(\mathbf{x})$ and the field $(2f_{NL}\Phi_l)$ which modulates the local power spectrum amplitude Δ_Φ . In principle, this should generate stochastic bias at order $\mathcal{O}(f_{NL}^2)$, but we will neglect this, since we are only calculating to order $\mathcal{O}(f_{NL})$.

Intuitively, in an f_{NL} cosmology, the local power spectrum amplitude Δ_Φ is not spatially constant, but varies throughout the universe in a way which is proportional to the long-wavelength potential Φ_l .

Computing the halo bias $b(k) = P_{mh}(k)/P_{mm}(k)$ from Eq. (17) for $n_l(\mathbf{x})$, we get:

$$\begin{aligned} b(k) &= \frac{b_1 P_{mm}(k) + \beta_f P_{m\Phi}(k)}{P_{mm}(k)} \\ &= b_1 + \frac{\beta_f f_{NL}}{\alpha(k, z)}. \end{aligned} \quad (20)$$

From the preceding argument, we predict that the scale-dependent f_{NL} bias is given by $\beta_f = 2(\partial \log n / \partial \log \Delta_\Phi)$. We will refer to this as a “weak” prediction for the bias: it cannot be used to constrain f_{NL} from real data, since β_f has not been expressed in terms of observable quantities.

To make further progress, we need to evaluate the derivative $(\partial \log n / \partial \log \Delta_\Phi)$, by making additional assumptions. If we assume that the halo mass function is universal, then one can calculate the derivative, obtaining $(\partial \log n / \partial \log \Delta_\Phi) = \delta_c(b_1 - 1)$, where b_1 is the Gaussian bias [28], so that:

$$\beta_f = 2\delta_c(b_1 - 1). \quad (21)$$

We will refer to this as a “strong” prediction for the scale-dependent bias in an f_{NL} cosmology, since β_f has been expressed in terms of the observable quantity b_1 . The strong form is essential for constraining f_{NL} from observations.

3.2 g_{NL} cosmology

Let us now generalize the analysis of large-scale clustering in the previous subsection to the case of a g_{NL} cosmology, with initial conditions given by:

$$\Phi(\mathbf{x}) = \Phi_G(\mathbf{x}) + g_{NL}(\Phi_G(\mathbf{x})^3 - 3\langle \Phi_G^2 \rangle \Phi_G(\mathbf{x})). \quad (22)$$

Separating the Gaussian field into long and short wavelength pieces $\Phi_G = \Phi_l + \Phi_s$, we decompose Φ as follows:

$$\begin{aligned} \Phi(\mathbf{x}) &= \underbrace{\Phi_l(\mathbf{x}) + g_{NL}(\Phi_l(\mathbf{x})^3 - 3\langle \Phi_l^2 \rangle \Phi_l(\mathbf{x}))}_{\text{long}} \\ &+ \underbrace{\Phi_s(\mathbf{x}) + 3g_{NL}(\Phi_l(\mathbf{x})^2 - \langle \Phi_l^2 \rangle) \Phi_s(\mathbf{x}) + 3g_{NL} \Phi_l(\mathbf{x})(\Phi_s(\mathbf{x})^2 - \langle \Phi_s^2 \rangle) + g_{NL}(\Phi_s(\mathbf{x})^3 - 3\langle \Phi_s^2 \rangle \Phi_s(\mathbf{x}))}_{\text{short}} \end{aligned} \quad (23)$$

As in the f_{NL} case, we’ll consider the perturbation to the long-wavelength halo density $n_h(\mathbf{x})$ generated by each of these terms.

The term $3g_{NL}(\Phi_l(\mathbf{x})^2 - \langle \Phi_l^2 \rangle) \Phi_s(\mathbf{x})$ can be interpreted as a local modulation in the small-scale power spectrum amplitude, given by $\Delta_\Phi \rightarrow (1 + 3g_{NL}(\Phi_l(\mathbf{x})^2 - \langle \Phi_l^2 \rangle)) \Delta_\Phi$. This generates a term $\Delta n_l(\mathbf{x}) = 3g_{NL}(\Phi_l(\mathbf{x})^2 - \langle \Phi_l^2 \rangle)(\partial n / \partial \log \Delta_\Phi)$ in the long-wavelength halo density, in close analogy with the f_{NL} case (the modulation is proportional to $g_{NL}(\Phi_l^2 - \langle \Phi_l^2 \rangle)$ in this case, rather than $f_{NL} \Phi_l$).

The term $3g_{NL} \Phi_l(\mathbf{x})(\Phi_s(\mathbf{x})^2 - \langle \Phi_s^2 \rangle)$ can be interpreted as follows. In a local region where the long-wavelength potential takes the value Φ_l , the small-scale modes are perturbed in the same way

as in an f_{NL} cosmology where the global value of f_{NL} is given by $(3g_{NL}\Phi_l)$. This generates a term $\Delta n_l(\mathbf{x}) = 3g_{NL}\Phi_l(\mathbf{x})(\partial n/\partial f_{NL})$ in the long-wavelength halo density.

Finally, there is the usual term $\Delta n_l(\mathbf{x}) = \delta_l(\mathbf{x})(\partial n/\partial \delta_l)$ due to changes in mean background density (as in the Gaussian case).

Putting this all together, we find that the long-wavelength halo density field in a g_{NL} cosmology is given by:⁴

$$\begin{aligned} n_l(\mathbf{x}) &= \bar{n} + \frac{\partial n}{\partial \delta_l} \delta_l(\mathbf{x}) + 3g_{NL} \frac{\partial n}{\partial \log \Delta_\Phi} (\Phi_l(\mathbf{x})^2 - \langle \Phi_l^2 \rangle) + 3g_{NL} \frac{\partial n}{\partial f_{NL}} \Phi_l(\mathbf{x}) \\ &= \bar{n} \left(1 + b_1 \delta_l(\mathbf{x}) + \frac{3}{2} \beta_f g_{NL} (\Phi_l(\mathbf{x})^2 - \langle \Phi_l^2 \rangle) + \beta_g g_{NL} \Phi_l(\mathbf{x}) \right) \end{aligned} \quad (24)$$

where b_1 and β_f were defined previously (Eqs. (18), (19)), and:

$$\beta_g = 3 \frac{\partial \log n}{\partial f_{NL}} \quad (25)$$

The large-scale halo bias $b(k) = P_{mh}(k)/P_{mm}(k)$ is given by:

$$b(k) = b_1 + \frac{\beta_g g_{NL}}{\alpha(k, z)}. \quad (26)$$

Note that the $(\beta_f g_{NL})$ term in Eq. (24) does not contribute to the bias, since the field $(\Phi_l(\mathbf{x})^2 - \langle \Phi_l^2 \rangle)$ and the long-wavelength density field δ_l are uncorrelated (their cross correlation is a three-point function of Gaussian fields, which vanishes). This term should generate stochastic bias, but we defer a systematic study of halo stochasticity in non-Gaussian cosmologies to a future paper [50].

We have now arrived at the peak-background split prediction (26) for halo bias in a g_{NL} cosmology, which relates the scale-dependent g_{NL} bias to the derivative $(\partial \log n/\partial f_{NL})$ of the halo mass function in an f_{NL} cosmology. In the terminology of the previous subsection, this is a “weak” prediction: we have shown that the problem of computing the g_{NL} bias is naturally related to the problem of understanding the mass function in an f_{NL} cosmology, but the coefficient β_g has not been expressed in terms of observable quantities.

To obtain a “strong” prediction, we need to evaluate the derivative $(\partial \log n/\partial f_{NL})$, which requires making additional assumptions. This has been done in [49], assuming a barrier crossing model for the mass function and using the Edgeworth expansion to calculate the derivative (see also [51–57]). The result is:

$$\frac{\partial \log n(M)}{\partial f_{NL}} = \frac{\kappa_3(M)}{6} H_3(\nu(M)) - \frac{1}{6} \frac{d\kappa_3/dM}{d\nu/dM} H_2(\nu(M)) \quad (27)$$

where $\nu = \delta_c/\sigma_M$, and $H_2(x) = x^2 - 1$ and $H_3(x) = x^3 - 3x$ are Hermite polynomials. We will compare this prediction with N -body simulations in §5.

⁴Analogously to the f_{NL} case, we have neglected two terms in Eq. (23). The term $g_{NL}(\Phi_l(\mathbf{x})^3 - 3\langle \Phi_l^2 \rangle \Phi_l(\mathbf{x}))$ only alters power spectra at order $\mathcal{O}(g_{NL}^2)$, and we will neglect terms of this order. The term $g_{NL}(\Phi_s(\mathbf{x})^3 - 3\langle \Phi_s^2 \rangle \Phi_s(\mathbf{x}))$ generates kurtosis in the density field and modifies the halo mass function [49], but in a way which is independent of Φ_l and therefore does not contribute to large-scale clustering.

4 Barrier crossing model

In this section, we will study large-scale bias using a barrier crossing model, obtaining results which are consistent with the peak-background split formalism from the previous section. The two approaches are complementary: the barrier model has the advantage that it generates complete predictions for halo statistics (such as the mass function or bias) via an algorithmic calculational procedure, but obscures the physical intuition of the peak-background split. For completeness, the calculations in this section will be sufficiently general to include the cases of Gaussian, f_{NL} -type, and g_{NL} -type initial conditions.

4.1 Setting up the calculation

The barrier crossing model is an old, widely influential idea in cosmology, in which halos of mass $\geq M$ are identified with peaks in the smoothed linear density field [58]. Although more complex versions have been proposed, we will use the simplest version: a spherical collapse model with constant barrier height, defined formally as follows.

We model halos of mass $\geq M$ as regions where the smoothed linear density field $\delta_M(\mathbf{x})$ (defined in Eq. (5)) exceeds the threshold value δ_c , i.e. the halo number density $n_h(\mathbf{x})$ is given by:

$$n_h(\mathbf{x}) = \frac{\rho_m}{M} \theta(\delta_M(\mathbf{x}) - \delta_c) \quad (28)$$

where θ is the step function

$$\theta(x) = \begin{cases} 0 & \text{if } x < 0 \\ 1 & \text{if } x \geq 0 \end{cases} \quad (29)$$

Throughout this paper, we take $\delta_c = 1.42$; this value produces somewhat improved agreement between the barrier model and simulations, compared to the Press-Schechter value $\delta_c = 1.69$.⁵

To study halo bias in this model, we define the following notation. Let \mathbf{x} , \mathbf{x}' be two points separated by distance r , let δ_{lin} denote the (unsmoothed) linear density field at \mathbf{x} , and let δ'_M denote the smoothed linear density field at \mathbf{x}' . We denote the joint PDF of these random variables by $p(\delta_{\text{lin}}, \delta'_M)$, and denote the 1-variable PDF of δ'_M by $p(\delta'_M)$. We define

$$p_0 = \int_{\delta_c}^{\infty} d\delta'_M p(\delta'_M) \quad (30)$$

$$\xi_0(r) = \int d\delta_{\text{lin}} d\delta'_M p(\delta_{\text{lin}}, \delta'_M) \delta_{\text{lin}} \theta(\delta'_M - \delta_c) \quad (31)$$

These quantities are related to the halo mass function $n(M)$ and matter-halo correlation function $\xi_{mh}(r)$, but there is one wrinkle. In the barrier crossing model, the field n_h defined in Eq. (28) represents the number density of halos with mass $\geq M$, whereas we want to consider a sample of halos with mass in a narrow mass range $(M, M + dM)$. Thus $n(M)$ and $\xi_{mh}(r)$ are obtained by

⁵We experimented with using a mass-dependent barrier $\delta_c(\nu)$ chosen for consistency with a universal mass function such as Sheth-Tormen [59] or Warren [60], but found that this did not result in further improvement.

taking derivatives as follows:

$$n(M) = -\frac{2\rho_m}{M} \left(\frac{dp_0}{dM} \right) \quad (32)$$

$$\xi_{mh}(r) = \frac{d\xi_0(r)/dM}{dp_0/dM} \quad (33)$$

4.2 Mass function, halo bias, and interpretation

In principle, calculation of the halo mass function and large-scale bias in the barrier crossing model has now been reduced to evaluation of Eqs. (30)–(33). We defer details of the calculation to Appendix A and quote the final results. The halo mass function is given by:

$$n(M) = \frac{2\rho_m}{M} \left(\frac{d \log \sigma^{-1}}{dM} \right) \frac{e^{-\nu^2/2}}{(2\pi)^{1/2}} \left[\nu + f_{NL} \left(\kappa_3^{(1)}(M) \frac{\nu H_3(\nu)}{6} - \frac{d\kappa_3^{(1)}/dM}{d(\log \sigma^{-1})/dM} \frac{H_2(\nu)}{6} \right) + g_{NL} \left(\kappa_4^{(1)}(M) \frac{\nu H_4(\nu)}{24} - \frac{d\kappa_4^{(1)}/dM}{d(\log \sigma^{-1})/dM} \frac{H_3(\nu)}{24} \right) \right] \quad (34)$$

The halo bias $b(k) = P_{mh}(k)/P_{mm}(k)$ is given by (in the large-scale limit $k \rightarrow 0$):

$$b(k) = b_1 + b_{1f} f_{NL} + b_{1g} g_{NL} + \frac{\beta_f f_{NL} + \beta_g g_{NL}}{\alpha(k)} \quad (35)$$

where:

$$b_1 = 1 + \frac{\nu^2 - 1}{\delta_c} \quad (36)$$

$$b_{1f} = -\kappa_3^{(1)}(M) \left(\frac{\nu^3 - \nu}{2\delta_c} \right) + \frac{d\kappa_3^{(1)}/dM}{d(\log \sigma^{-1})/dM} \left(\frac{\nu + \nu^{-1}}{6\delta_c} \right) \quad (37)$$

$$b_{1g} = -\kappa_4^{(1)}(M) \left(\frac{\nu^4 - 3\nu^2}{6\delta_c} \right) + \frac{d\kappa_4^{(1)}/dM}{d(\log \sigma^{-1})/dM} \left(\frac{\nu^2}{12\delta_c} \right) \quad (38)$$

$$\beta_f = 2\nu^2 - 2 \quad (39)$$

$$\beta_g = \kappa_3^{(1)}(M) \frac{\nu^3 - 3\nu}{2} - \frac{d\kappa_3^{(1)}/dM}{d(\log \sigma^{-1})/dM} \left(\frac{\nu - \nu^{-1}}{2} \right) \quad (40)$$

Although the above expressions are the result of a purely formal calculation, we will now show that each term has a natural interpretation.

Considering first the halo mass function (34), we have found a Press-Schechter mass function (with $\delta_c = 1.42$) in the Gaussian case, plus first-order corrections in f_{NL} and g_{NL} which agree with those found in [49, 52] using the Edgeworth expansion. This agreement is expected since the two calculations are based on the same barrier crossing model.

Moving on to halo bias, in the Gaussian case, we predict that $b(k)$ is constant on large scales, with value b_1 given by Eq. (36). The peak-background split argument suggests a general relation between the large-scale halo bias and the halo mass function which applies generally to a universal mass function of the form:

$$n(M) = \frac{\rho_m}{M} f(\nu) \frac{d \log \sigma^{-1}}{dM} \quad (41)$$

On large scales, the bias is predicted to be scale-independent and given by [61]:

$$b_1 = 1 - \frac{\nu}{\delta_c} \frac{d \log f}{d\nu} \quad (42)$$

Comparing our predictions (34), (36) for $n(M)$ and b_1 , we find agreement, i.e. Eq. (36) for b_1 can be interpreted as the general peak-background split expression for halo bias, specialized to the Press-Schechter mass function.

More generally, the b_{1f} and b_{1g} contributions to the bias (Eqs. (37), (38)) represent shifts in the scale-independent part of the bias due to primordial non-Gaussianity. It is straightforward to check that these terms can be obtained by plugging the non-Gaussian mass function in Eq. (34) into the peak-background split prediction (42) for scale-independent bias, i.e. the b_{1f} and b_{1g} terms can be interpreted as changes to the bias which are entirely due to the mass function being perturbed in a non-Gaussian cosmology. This type of term (scale-independent bias proportional to f_{NL}) was first found for f_{NL} cosmologies in [30]. Note that a scale-independent shift is unobservable in practice, and cannot be used to constrain non-Gaussianity, since the bias of a real tracer population, such as galaxies or quasars, is a free parameter.

The β_f contribution to the bias is the well-known scale-dependent bias in an f_{NL} cosmology. Comparing Eq. (39) for β_f with Eqs. (34), (36), this term can be written either as $\beta_f = 2\partial(\log n)/\partial(\log \Delta_\Phi)$ or $\beta_f = 2\delta_c(b_1 - 1)$. (In §3, we referred to these as “weak” and “strong” predictions.)

The β_g contribution to the bias is the focus of this paper: scale-dependent bias in a g_{NL} cosmology. Eq. (40) gives this term in the “strong” form that was found previously (Eq. (27)) using the peak-background split argument. Alternately, we can write this term in the “weak” form $\beta_g = 3\partial(\log n)/\partial f_{NL}$ using Eq. (34).

In summary, we have found that the complete expression for large-scale halo bias in the barrier crossing model (Eq. (35)) agrees perfectly with the peak-background split calculation from §3. The bias contains a scale-independent part ($b_1 + b_{1f}f_{NL} + b_{1g}g_{NL}$) which can be obtained from the halo mass function, via the general relation (42). The scale-independent bias depends on f_{NL} and g_{NL} , because the halo mass function depends on these parameters. The bias also contains a scale-dependent part $(\beta_f f_{NL} + \beta_g g_{NL})/\alpha(k)$ whose coefficients can be calculated explicitly and agree with the peak-background split predictions.

4.3 Comparison with previous work

It is interesting to compare the above calculations with the results of [62] (see also [43]), where β_g was calculated using the MLB formula [63], which gives N -point functions of halos as an asymptotic series in ν . The scale-dependent g_{NL} bias was found to be (in our notation):

$$\beta_g^{\text{MLB}} = \kappa_3^{(1)}(M) \frac{\delta_c \nu (b_1 - 1)}{2} \quad (43)$$

When this prediction was compared to N -body simulations, it was found to be a poor fit.

Comparing β_g^{MLB} with our calculation (40) for β_g , it is seen that the two agree in the high-mass limit $\nu \rightarrow \infty$, but disagree in subleading terms. This is expected since the MLB formula is based on

the same barrier crossing model that we have used, but it is an asymptotic result, whereas we have done an exact calculation (to first order in f_{NL} , g_{NL}). For realistic halo masses, the “subleading” terms neglected in the MLB formula are of order one (to quantify this better, β_g and β_g^{MLB} agree to 10% only when the halo bias $b_1 \geq 15$), so in practice the two predictions are quite different.

Recently, ref. [46] argued that the barrier crossing model cannot generate correct predictions for general non-Gaussian initial conditions such as the g_{NL} model, but we found the opposite conclusion: brute-force calculation in the barrier crossing model, collecting all terms of order $\mathcal{O}(g_{NL})$, agrees precisely (i.e. to all orders in $1/\nu$) with the peak-background split. It seems intuitively plausible that two must be consistent, since the peak-background split argument depends only on the assumption that halo formation is determined by the local density field, and the barrier crossing model is a concrete example of a model in which this assumption is satisfied.

5 Results from N -body simulations

In the last two sections, we have obtained complete analytic predictions for large-scale bias in a g_{NL} cosmology, finding agreement between the peak-background split formalism (§3) and a barrier crossing model based on spherical collapse (§4).

To compare these predictions with simulation, we performed collisionless N -body simulations using the GADGET-2 TreePM code [64]. Simulations were done using periodic box size $R_{\text{box}} = 1600 h^{-1}$ Mpc, particle count $N_p = 1024^3$, and force softening length $R_s = 0.05(R_{\text{box}}/N_p^{1/3})$. With these parameters and the fiducial cosmology from §1, the particle mass is $m_p = 2.92 \times 10^{11} h^{-1} M_{\odot}$.

We generate initial conditions by simulating a Gaussian primordial potential Φ , and applying f_{NL} or g_{NL} corrections by straightforward use of Eq. (1). We linearly evolve to redshift $z_{\text{ini}} = 100$ using the transfer function⁶ from CAMB [48], and obtain initial particle positions at this redshift using the Zeldovich approximation [65]. (At $z_{\text{ini}} = 100$, transient effects due to use of this approximation should be negligible [66].)

After running the N -body simulation, we group particles into halos using an MPI parallelized implementation of the friends-of-friends algorithm [67] with link length $L_{\text{FOF}} = 0.2R_{\text{box}}N_p^{-1/3}$. For a halo containing N_{FOF} particles, we assign a halo position given by the mean of the individual particle positions. We estimate halo bias $b(k) = P_{mh}(k)/P_{mm}(k)$ using the procedure described in Appendix A of [68]. The statistical error $\Delta b(k)$ obtained using this procedure is smaller than the error that would be obtained assuming uncorrelated estimates of the power spectra P_{mm} and P_{mh} , since shared sample variance is taken into account.

Results in this paper are based on 4 simulations with Gaussian initial conditions, 5 simulations with $g_{NL} = \pm 2 \times 10^6$, and 3 simulations with $f_{NL} = \pm 250$ (for a total of 20 simulations).

⁶One subtlety here: straightforward use of CAMB’s transfer function at redshift 100 leads to inconsistencies since CAMB includes radiation (which is not negligible at $z = 100$) in its expansion history, while GADGET does not. For this reason we use CAMB’s linear transfer function at low redshift and extrapolate back to $z = 100$ using the growth function in an $\Omega_{\text{rad}} = 0$ universe.

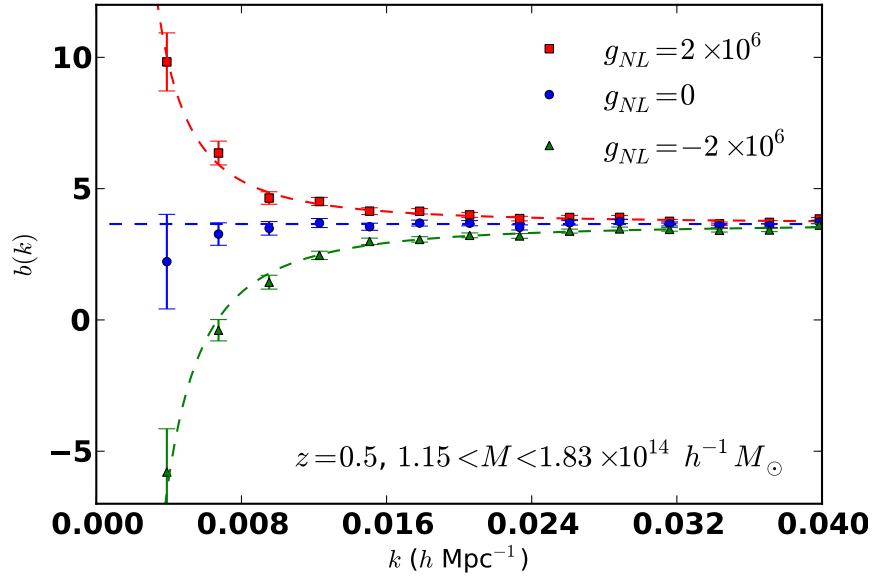


Figure 1: An example to illustrate that halo bias in a g_{NL} cosmology takes the functional form $b(k) = b_1 + \beta_g g_{NL}/\alpha(k)$. This figure corresponds to redshift $z = 0.5$ and halo mass range $1.15 \leq M \leq 1.83 \times 10^{14} h^{-1} M_\odot$, but we find the same functional form for all redshifts and halo masses.

5.1 Fitting the functional form $b(k) = b_1 + \beta_g g_{NL}/\alpha(k)$

We now compare our analytic prediction for $b(k)$ to simulation in several steps, corresponding to increasingly strong versions of the prediction.

First, consider the weakest possible question: our analytic prediction for the bias is of the functional form

$$b(k) = b_1 + \beta_g \frac{g_{NL}}{\alpha(k)} \quad (44)$$

Is this a good fit to simulation, if we treat the coefficients b_1 and β_g as free parameters? (We will compare our analytic prediction for β_g to simulation in the next subsection; for now we are just testing whether the functional form (44) is correct.)

In Fig. 1, we show some example fits of this form, for redshift $z = 0.5$ and halo mass range $1.15 \leq M \leq 1.83 \times 10^{14} h^{-1} M_\odot$. Each fit was performed using bias estimates from 4 independent simulations with $L_{\text{box}} = 1600 h^{-1} \text{Mpc}$ and wavenumbers $k \leq 0.04 h \text{Mpc}^{-1}$. We find good χ^2 values for the fits, with recovered parameters:

$$\begin{aligned} b_1 &= 3.653 \pm 0.026 && \text{for } g_{NL} = 0 \\ (b_1, 10^3 \beta_g) &= (3.575 \pm 0.038, 0.581 \pm 0.056) && \text{for } g_{NL} = 2 \times 10^6 \\ (b_1, 10^3 \beta_g) &= (3.824 \pm 0.039, 0.935 \pm 0.060) && \text{for } g_{NL} = -2 \times 10^6 \end{aligned} \quad (45)$$

We note that the recovered bias parameters (45) in this example show that both b_1 and β_g are g_{NL} -dependent. In the barrier crossing model, we made a prediction for the g_{NL} dependence of

b_1 (Eq. (38)). We find good agreement between this prediction and our simulations. Note that in practice, the g_{NL} dependence of b_1 is unobservable since for a real tracer population, the halo occupation distribution is not known precisely and b_1 must be treated as a free parameter to be determined from data.

The observed g_{NL} dependence of β_g corresponds to scale-dependent bias of order $\mathcal{O}(g_{NL}^2)$ or higher (note that β_g is defined in such a way that constant β_g corresponds to scale-dependent bias which is linear in g_{NL}). This complicates comparison with our analytic predictions, since we have only calculated the bias to order $\mathcal{O}(g_{NL})$. We address this by estimating β_g by averaging the estimates obtained from simulations with $g_{NL} = \pm 2 \times 10^6$, thus removing contributions to $b(k)$ which are proportional to g_{NL}^2 . Note that this does not remove $\mathcal{O}(g_{NL}^3)$ contributions to the bias, but we have checked that such contributions are negligible for $g_{NL} = \pm 2 \times 10^6$, by comparing with simulations with halved step size.

Repeating this fitting procedure for redshifts $z \in \{2, 1, 0.5, 0\}$ and a range of halo masses (the precise set of halo mass bins used is shown in Fig. 2 below), we find χ^2 values which are consistent with their expected distribution, i.e. we find that the functional form (44) is a good fit to the simulations for a wide range of redshifts and halo masses. For this reason, in subsequent sections, we will “compress” the estimates of $b(k)$ in each simulation (as shown in Fig. 1) to two numbers (b_1 and β_g), with statistical errors given by the fitting procedure.

5.2 Comparison with analytic predictions

Now that we have established the functional form $b(k) = b_1 + \beta_g g_{NL} / \alpha(k)$ of the bias, and a procedure for estimating β_g from simulation as a function of redshift and halo mass, we would like to compare with our analytic predictions for β_g .

First, consider the “weak” form of the prediction ($\beta_g = 3(\partial \log n / \partial f_{NL})$) obtained from the peak-background split argument. We can test this prediction by estimating the derivative ($\partial \log n / \partial f_{NL}$) directly from simulations, by taking finite differences of $\log(n)$ in simulations with $f_{NL} = \pm 250$. (We checked convergence in the step size.) We find that the prediction holds perfectly (within the statistical errors of the simulations) for all redshifts and halo masses (Fig. 2).

Second, consider the “strong” Edgeworth prediction (Eq. (40)), in which an explicit formula for β_g is given. In this case, we find reasonable agreement at high mass ($M \gtrsim 10^{14} h^{-1} M_\odot$), but the prediction breaks down at low halo mass (Fig. 2).

Our interpretation is as follows. The peak-background split prediction $\beta_g = 3(\partial \log n / \partial f_{NL})$ is a universal relation between bias in a g_{NL} cosmology and the mass function in an f_{NL} cosmology. Although “weak” in the sense that it does not supply a closed-form expression for β_g , the derivation makes few assumptions, and one expects it to be exact. In order to constrain g_{NL} from real data, we need a “strong” prediction which expresses β_g in closed form, using only observable quantities (i.e. the analog of the Dalal et al formula $\beta_f = 2\delta_c(b_1 - 1)$ for an f_{NL} cosmology). Using the Edgeworth expansion, one can make such a prediction in the context of the barrier crossing model (Eq. (40)), and obtain rough agreement with simulations, but the level of agreement is not really good enough for doing precision cosmology. Therefore, we next propose a slightly modified version of the Edgeworth prediction.

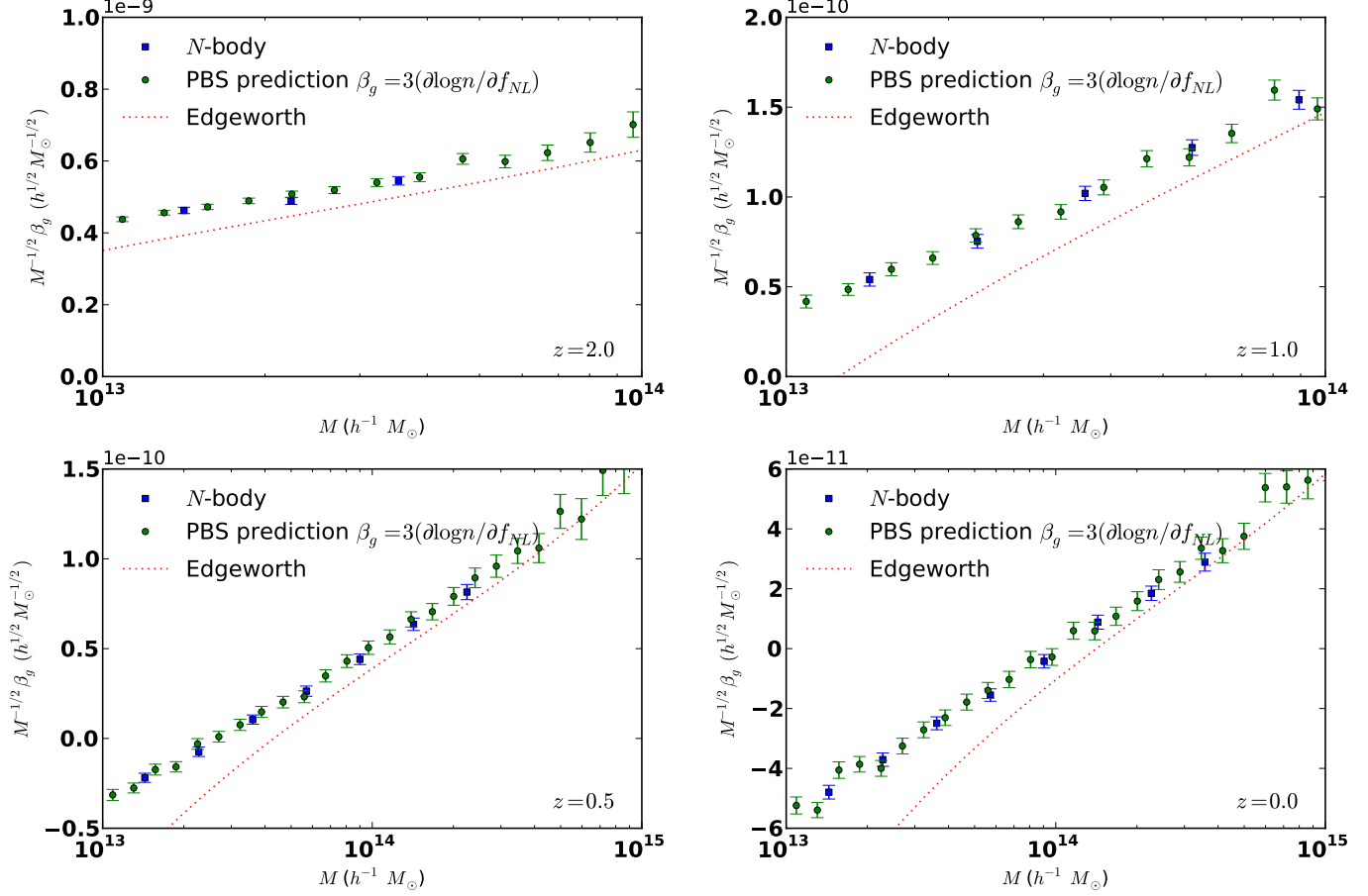


Figure 2: Comparison of the “weak” and “strong” predictions for the scale-dependent bias in a g_{NL} cosmology. **Blue squares:** Direct estimates of the bias, extracted from simulations with $g_{NL} = \pm 2 \times 10^6$ as described in §5.1. **Green circles:** “Weak” analytic prediction for the bias ($\beta_g = 3(\partial \log n / \partial f_{NL})$) from the peak-background split formalism, showing perfect agreement. The estimates of $(\partial \log n / \partial f_{NL})$ shown in the figure were obtained directly from simulations with $f_{NL} = \pm 250$. **Red dotted curve:** Edgeworth prediction for the bias (Eq. (40)). Good agreement is seen at high mass, but at low masses Edgeworth underpredicts $3(d \log n / df_{NL})$. We will find an improvement in §5.3.

5.3 A simple universal formula for the bias in a g_{NL} cosmology

We would like to slightly modify the Edgeworth prediction (40) for β_g so that it agrees better with N -body simulations. It is also convenient to have a prediction in which β_g is given as a function of observable quantities: Gaussian bias b_1 (rather than halo mass, which is unobservable) and redshift z .

We start by rewriting the Edgeworth prediction (40) for β_g in terms of variables (b_1, z) . The following fitting functions for κ_3 and $d\kappa_3/d\log(\sigma^{-1})$ are convenient:

$$\kappa_3 = 0.000329(1 + 0.09z)b_1^{-0.09} \quad (46)$$

$$\frac{d\kappa_3}{d\log\sigma^{-1}} = -0.000061(1 + 0.22z)b_1^{-0.25} \quad (47)$$

For purposes of this subsection, we *define* the quantity ν to be given in terms of b_1 and z by:

$$\nu = [\delta_c(b_1 - 1) + 1]^{1/2} \quad (\text{where } \delta_c = 1.42) \quad (48)$$

The Edgeworth prediction for β_g can be written in the following form:

$$\beta_g^{\text{Edge.}} = \kappa_3 \left[-1 + \frac{3}{2}(\nu - 1)^2 + \frac{1}{2}(\nu - 1)^3 \right] - \frac{d\kappa_3}{d\log\sigma^{-1}} \left(\frac{\nu - \nu^{-1}}{2} \right) \quad (49)$$

Empirically, we find that if we tweak the Edgeworth prediction by changing the coefficients of the polynomial in brackets as follows:

$$\beta_g = \kappa_3 \left[-0.7 + 1.4(\nu - 1)^2 + 0.6(\nu - 1)^3 \right] - \frac{d\kappa_3}{d\log\sigma^{-1}} \left(\frac{\nu - \nu^{-1}}{2} \right) \quad (50)$$

then we obtain good agreement with simulations (Fig. 3). The expression (50) for β_g (with quantities κ_3 , $d\kappa_3/d\log\sigma^{-1}$, ν defined by Eqs. (46)–(48)) is one of the main results of this paper and is our observational “bottom line” when constraining g_{NL} from real data.

We have motivated our “tweak” to the Edgeworth prediction as essentially a fitting function for the ν dependence (although it is worth noting that the z dependence is correctly predicted by the barrier crossing model). A speculative interpretation of this tweak, which we will defer for future work, is as follows. In the barrier crossing model, the second-order halo bias is given by $b_2 = (\nu^3 - 3\nu)/(\delta_c\sigma_M)$. It is tempting to conjecture that the expression in brackets in Eq. (50) is generally equal to $(\delta_c\sigma_M b_2)$, and interpret our “tweak” to the Edgeworth prediction (49) as perturbing the relation between b_1 and b_2 , relative to the barrier crossing model. This opens up the possibility of directly measuring the second-order bias and determining β_g directly. To study the viability of this idea, one would need to compare β_g in simulation to some other estimate of second-order halo bias, such as the halo bispectrum in the squeezed limit.

5.4 An important caveat

There is an important caveat when using Eq. (50), or indeed any fitting function for the g_{NL} bias, to constrain g_{NL} from real data. It is tempting to compute β_g by simply plugging the observed bias b_1

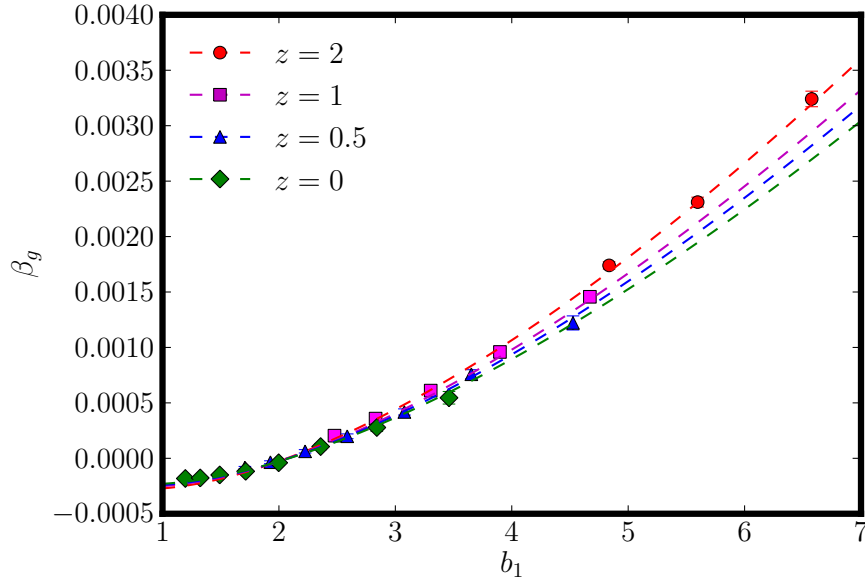


Figure 3: Scale-dependent g_{NL} bias coefficient β_g as a function of redshift z and halo bias b_1 , showing excellent agreement between our final analytic result (Eq. (50), dashed curves) and N -body simulations (error bars).

and redshift z into Eq. (50). (Since the z -dependence is very mild, a rough estimate for the redshift suffices.) However, we have only shown that this procedure is correct in the limit of a narrow bin in halo mass and redshift, and a real tracer population will be a weighted average over M and z .

For example, consider the case in which the “tracers” are the dark matter particles themselves, i.e. each halo is weighted in proportion to its mass (assuming all mass is in halos). This tracer population has bias $b_1 = 1$ (for the trivial reason that we are back to the dark matter field), so straightforward use of Eq. (50) would suggest that $\beta_g \approx -0.00025$. (This value would make the low- k power spectrum a reasonably sensitive probe of g_{NL} .) In fact, the true β_g of this tracer is zero, since the matter power spectrum $P_{mm}(k)$ does not contain a term proportional to $g_{NL}/\alpha(k)$. This example shows that the true g_{NL} bias of a tracer population can differ significantly from the value obtained by straightforward use of Eq. (50). In general, the g_{NL} bias will depend on the full HOD (halo occupation distribution) of the tracer population, not only on the Gaussian bias b_1 .⁷

One popular approach to modeling the HOD is to assume that halos below some minimum mass M_{\min} do not host tracers, whereas the mean number of tracers in a halo of mass $M \geq M_{\min}$ is proportional to the total mass M . For reference, we give a fitting function for the g_{NL} bias for this HOD:

$$\beta_g = \kappa_3 \left[-0.4(\nu - 1) + 1.5(\nu - 1)^2 + 0.6(\nu - 1)^3 \right] \quad (51)$$

where for purposes of this equation, κ_3 and ν are defined as functions of the observables b_1 and z

⁷Note that there is no analogous caveat in the f_{NL} case. Because the relation $\beta_f = 2\delta_c(b_1 - 1)$ is linear, it applies to both a tracer population which is narrowly selected in (M, z) and to a population which is an arbitrary weighted average over (M, z) .

by Eqs. (46), (48) above.

Eq. (51) applies to a mass-weighted population of halos above M_{\min} , whereas Eq. (50) applies to a population which is narrowly selected in mass. The two agree for $b_1 \gtrsim 2.5$, suggesting that HOD dependence is small in practice for highly biased samples, but disagree qualitatively for $b_1 \lesssim 2.5$. For example, the g_{NL} bias β_g changes sign at $b_1 \approx 2.1$ for the narrowly selected sample (Eq. (50)), whereas β_g is always positive for the mass-weighted sample (Eq. (51)).

Our perspective is that, in order to obtain g_{NL} constraints which are robust to HOD modeling uncertainty, one should use highly biased samples ($b_1 \gtrsim 2.5$), where this uncertainty will be minimized. Samples which are not highly biased do not give robust constraints; for example, a tracer population with $b_1 = 1.8$ can have a g_{NL} bias β_g which is negative, zero, or positive, depending on the HOD.

For highly biased samples, it is useful to make the following observation: the g_{NL} bias β_g^{fit} which is obtained from straightforward use of Eq. (50) is always less than the true g_{NL} bias β_g^{true} .⁸ This follows from positivity of the second derivative $d^2\beta_g/db_1^2$. It follows that a g_{NL} constraint obtained using β_g^{fit} is always valid, but slightly overestimates the statistical error that could be obtained if β_g^{true} were known. This effectively treats HOD uncertainty as an extra source of systematic error.

6 Discussion

We have computed large-scale halo bias for non-Gaussian initial conditions, using two analytic frameworks: the peak-background split formalism (§3) and a barrier crossing model (§4), finding agreement between the two. Although our emphasis has been on the constant- f_{NL} and constant- g_{NL} models, our calculational machinery should apply to more general non-Gaussian initial conditions.

The peak-background split formalism is simpler and also suggests a simple physical picture of non-Gaussian cosmologies on large scales. In an f_{NL} cosmology, the amplitude Δ_Φ of the initial fluctuations is not spatially constant, but is proportional to $(1 + 2f_{NL}\Phi_l)$. Thus, Δ_Φ has fluctuations on large scales which are 100% correlated with the long-wavelength potential, generating halo bias of the form $(\beta_f f_{NL}/\alpha(k))$. In a g_{NL} cosmology, the small-scale skewness is nonzero and proportional to $(g_{NL}\Phi_l)$, leading to halo bias of the form $(\beta_g g_{NL}/\alpha(k))$. The peak-background split argument is very useful for generating universal relations such as $\beta_g = 3\partial(\log n)/\partial f_{NL}$, which are “weak” in the sense that the RHS has not been expressed in terms of observable quantities, but have the advantage of being exact (as can be seen by comparing the two sets of errorbars in Fig. 2).

The barrier crossing model generates all terms in the large-scale bias, including terms such as b_{1f} and b_{1g} which are easy to miss, by a purely algorithmic calculational procedure. In addition, the barrier crossing model generates “strong” forms of the bias coefficients (e.g. the Edgeworth expression (40) for β_g), which are closed-form expressions in M and z . However, these expressions are not exact because the barrier crossing model is approximation to the true process of halo formation.

⁸This statement assumes that the probability that a halo hosts a tracer is a function only of the mass and redshift. If the probability depends strongly on additional variables such as merger history, triaxiality, etc. then this will generate additional contributions to β_g , in analogy to the f_{NL} case [28, 69]. In principle, selection biases to β_g can be addressed by folding the selection into the mass function when computing $\partial(\log n)/\partial f_{NL}$, but detailed study is beyond the scope of this paper.

To obtain a “bottom line” expression for the scale-dependent g_{NL} bias β_g in terms of redshift z and Gaussian bias z , we found it necessary to tweak slightly the b_1 dependence of the Edgeworth prediction, arriving at the expression (50) which agrees very well with simulations. The caveat is that Eq. (50) applies only to a halo population which has been selected in a narrow halo mass and redshift range. In principle, one can calculate β_g for a tracer population by multiplying by the halo occupation distribution and integrating over mass and redshift. In practice, the HOD is not known precisely and we have argued in §5.4 that the best approach is to only use highly biased populations ($b \gtrsim 2.5$) for constraining g_{NL} . Since β_g is a rapidly increasing function of b_1 , this strategy makes sense both from the perspective of minimizing statistical errors, and systematic errors due to HOD uncertainty. In data analysis, it may be useful to impose cuts which increase the mean halo bias at the expense of reducing the number of tracers. Another advantage of subdividing tracer populations is that this may permit f_{NL} and g_{NL} to be constrained simultaneously (with a single tracer population, the two are degenerate).

Acknowledgements

We thank Neal Dalal, Vincent Desjacques, Chris Hirata, Donghui Jeong, Brant Robertson, Fabian Schmidt, Neelima Sehgal, David Spergel and Matias Zaldarriaga for helpful discussions. K. M. S. is supported by a Lyman Spitzer fellowship in the Department of Astrophysical Sciences at Princeton University. M. L. is supported as a Friends of the Institute for Advanced Study Member and by the NSF through AST-0807444. S. F. is supported by the Martin Schwarzschild Fund in Astronomy at Princeton University. Simulations in this paper were performed at the TIGRESS high performance computer center at Princeton University which is jointly supported by the Princeton Institute for Computational Science and Engineering and the Princeton University Office of Information Technology.

References

- [1] E. Komatsu *et al.*, “Seven-Year Wilkinson Microwave Anisotropy Probe (WMAP) Observations: Cosmological Interpretation,” arXiv:1001.4538 [astro-ph.CO].
- [2] SDSS Collaboration, W. J. Percival *et al.*, “Baryon Acoustic Oscillations in the Sloan Digital Sky Survey Data Release 7 Galaxy Sample,” *Mon. Not. Roy. Astron. Soc.* **401** (2010) 2148–2168, arXiv:0907.1660 [astro-ph.CO].
- [3] B. A. Reid *et al.*, “Cosmological Constraints from the Clustering of the Sloan Digital Sky Survey DR7 Luminous Red Galaxies,” *Mon. Not. Roy. Astron. Soc.* **404** (2010) 60–85, arXiv:0907.1659 [astro-ph.CO].
- [4] A. G. Riess *et al.*, “A 3% Solution: Determination of the Hubble Constant with the Hubble Space Telescope and Wide Field Camera 3,” *Astrophys. J.* **730** (2011) 119, arXiv:1103.2976 [astro-ph.CO].

- [5] R. Kessler *et al.*, “First-year Sloan Digital Sky Survey-II (SDSS-II) Supernova Results: Hubble Diagram and Cosmological Parameters,” *Astrophys. J. Suppl.* **185** (2009) 32–84, arXiv:0908.4274 [astro-ph.CO].
- [6] A. Vikhlinin *et al.*, “Chandra Cluster Cosmology Project III: Cosmological Parameter Constraints,” *Astrophys. J.* **692** (2009) 1060–1074, arXiv:0812.2720 [astro-ph].
- [7] A. H. Guth, “The Inflationary Universe: A Possible Solution to the Horizon and Flatness Problems,” *Phys. Rev.* **D23** (1981) 347–356.
- [8] A. D. Linde, “Chaotic Inflation,” *Phys. Lett.* **B129** (1983) 177–181.
- [9] A. Albrecht and P. J. Steinhardt, “Cosmology for Grand Unified Theories with Radiatively Induced Symmetry Breaking,” *Phys. Rev. Lett.* **48** (1982) 1220–1223.
- [10] A. H. Guth and S. Y. Pi, “Fluctuations in the New Inflationary Universe,” *Phys. Rev. Lett.* **49** (1982) 1110–1113.
- [11] S. W. Hawking, “The Development of Irregularities in a Single Bubble Inflationary Universe,” *Phys. Lett.* **B115** (1982) 295.
- [12] A. A. Starobinsky, “Dynamics of Phase Transition in the New Inflationary Universe Scenario and Generation of Perturbations,” *Phys. Lett.* **B117** (1982) 175–178.
- [13] J. M. Bardeen, P. J. Steinhardt, and M. S. Turner, “Spontaneous Creation of Almost Scale - Free Density Perturbations in an Inflationary Universe,” *Phys. Rev.* **D28** (1983) 679.
- [14] D. S. Salopek and J. R. Bond, “Nonlinear evolution of long wavelength metric fluctuations in inflationary models,” *Phys. Rev.* **D42** (1990) 3936–3962.
- [15] A. Gangui, F. Lucchin, S. Matarrese, and S. Mollerach, “The Three point correlation function of the cosmic microwave background in inflationary models,” *Astrophys. J.* **430** (1994) 447–457, arXiv:astro-ph/9312033.
- [16] E. Komatsu and D. N. Spergel, “Acoustic signatures in the primary microwave background bispectrum,” *Phys. Rev.* **D63** (2001) 063002, arXiv:astro-ph/0005036.
- [17] T. Okamoto and W. Hu, “The Angular Trispectra of CMB Temperature and Polarization,” *Phys. Rev.* **D66** (2002) 063008, arXiv:astro-ph/0206155.
- [18] A. D. Linde and V. F. Mukhanov, “Nongaussian isocurvature perturbations from inflation,” *Phys. Rev.* **D56** (1997) 535–539, arXiv:astro-ph/9610219.
- [19] D. H. Lyth and D. Wands, “Generating the curvature perturbation without an inflaton,” *Phys. Lett.* **B524** (2002) 5–14, arXiv:hep-ph/0110002.
- [20] D. H. Lyth, C. Ungarelli, and D. Wands, “The primordial density perturbation in the curvaton scenario,” *Phys. Rev.* **D67** (2003) 023503, arXiv:astro-ph/0208055.

- [21] G. Dvali, A. Gruzinov, and M. Zaldarriaga, “A new mechanism for generating density perturbations from inflation,” *Phys. Rev.* **D69** (2004) 023505, arXiv:astro-ph/0303591.
- [22] L. Kofman, “Probing string theory with modulated cosmological fluctuations,” arXiv:astro-ph/0303614.
- [23] E. I. Buchbinder, J. Khoury, and B. A. Ovrut, “Non-Gaussianities in New Ekpyrotic Cosmology,” *Phys. Rev. Lett.* **100** (2008) 171302, arXiv:0710.5172 [hep-th].
- [24] P. Creminelli and L. Senatore, “A smooth bouncing cosmology with scale invariant spectrum,” *JCAP* **0711** (2007) 010, arXiv:hep-th/0702165.
- [25] J.-L. Lehners and P. J. Steinhardt, “Non-Gaussian Density Fluctuations from Entropically Generated Curvature Perturbations in Ekpyrotic Models,” *Phys. Rev.* **D77** (2008) 063533, arXiv:0712.3779 [hep-th].
- [26] J. M. Maldacena, “Non-Gaussian features of primordial fluctuations in single field inflationary models,” *JHEP* **05** (2003) 013, arXiv:astro-ph/0210603.
- [27] P. Creminelli and M. Zaldarriaga, “Single field consistency relation for the 3-point function,” *JCAP* **0410** (2004) 006, arXiv:astro-ph/0407059.
- [28] A. Slosar, C. Hirata, U. Seljak, S. Ho, and N. Padmanabhan, “Constraints on local primordial non-Gaussianity from large scale structure,” *JCAP* **0808** (2008) 031, arXiv:0805.3580 [astro-ph].
- [29] J. R. Fergusson, D. M. Regan, and E. P. S. Shellard, “Optimal Trispectrum Estimators and WMAP Constraints,” arXiv:1012.6039 [astro-ph.CO].
- [30] V. Desjacques, U. Seljak, and I. Iliev, “Scale-dependent bias induced by local non-Gaussianity: A comparison to N-body simulations,” arXiv:0811.2748 [astro-ph].
- [31] M. Sasaki, J. Valiviita, and D. Wands, “Non-gaussianity of the primordial perturbation in the curvaton model,” *Phys. Rev.* **D74** (2006) 103003, arXiv:astro-ph/0607627.
- [32] K. Ichikawa, T. Suyama, T. Takahashi, and M. Yamaguchi, “Non-Gaussianity, Spectral Index and Tensor Modes in Mixed Inflation and Curvaton Models,” *Phys. Rev.* **D78** (2008) 023513, arXiv:0802.4138 [astro-ph].
- [33] K. Enqvist and T. Takahashi, “Signatures of Non-Gaussianity in the Curvaton Model,” *JCAP* **0809** (2008) 012, arXiv:0807.3069 [astro-ph].
- [34] Q.-G. Huang, “Curvaton with Polynomial Potential,” *JCAP* **0811** (2008) 005, arXiv:0808.1793 [hep-th].
- [35] P. Chingangbam and Q.-G. Huang, “The Curvature Perturbation in the Axion-type Curvaton Model,” *JCAP* **0904** (2009) 031, arXiv:0902.2619 [astro-ph.CO].

- [36] Q.-G. Huang, “A geometric description of the non-Gaussianity generated at the end of multi-field inflation,” *JCAP* **0906** (2009) 035, arXiv:0904.2649 [hep-th].
- [37] C. T. Byrnes and G. Tasinato, “Non-Gaussianity beyond slow roll in multi-field inflation,” *JCAP* **0908** (2009) 016, arXiv:0906.0767 [astro-ph.CO].
- [38] N. Dalal, O. Dore, D. Huterer, and A. Shirokov, “The imprints of primordial non-gaussianities on large- scale structure: scale dependent bias and abundance of virialized objects,” *Phys. Rev. D* **77** (2008) 123514, arXiv:0710.4560 [astro-ph].
- [39] J.-Q. Xia, C. Baccigalupi, S. Matarrese, L. Verde, and M. Viel, “Constraints on Primordial Non-Gaussianity from Large Scale Structure Probes,” arXiv:1104.5015 [astro-ph.CO].
- [40] C. Cunha, D. Huterer, and O. Dore, “Primordial non-Gaussianity from the covariance of galaxy cluster counts,” *Phys. Rev. D* **82** (2010) 023004, arXiv:1003.2416 [astro-ph.CO].
- [41] N. Hamaus, U. Seljak, and V. Desjacques, “Optimal Constraints on Local Primordial Non-Gaussianity from the Two-Point Statistics of Large-Scale Structure,” arXiv:1104.2321 [astro-ph.CO].
- [42] S. Matarrese and L. Verde, “The effect of primordial non-Gaussianity on halo bias,” *Astrophys. J.* **677** (2008) L77, arXiv:0801.4826 [astro-ph].
- [43] T. Giannantonio and C. Porciani, “Structure formation from non-Gaussian initial conditions: multivariate biasing, statistics, and comparison with N- body simulations,” *Phys. Rev. D* **81** (2010) 063530, arXiv:0911.0017 [astro-ph.CO].
- [44] M. Grossi, K. Dolag, E. Branchini, S. Matarrese, and L. Moscardini, “Evolution of Massive Haloes in non-Gaussian Scenarios,” *Mon. Not. Roy. Astron. Soc.* **382** (2007) 1261, arXiv:0707.2516 [astro-ph].
- [45] A. Pillepich, C. Porciani, and O. Hahn, “Universal halo mass function and scale-dependent bias from N-body simulations with non-Gaussian initial conditions,” arXiv:0811.4176 [astro-ph].
- [46] V. Desjacques, D. Jeong, and F. Schmidt, “Non-Gaussian Halo Bias Re-examined: Mass-dependent Amplitude from the Peak-Background Split and Thresholding,” arXiv:1105.3628 [astro-ph.CO].
- [47] WMAP Collaboration, J. Dunkley *et al.*, “Five-Year Wilkinson Microwave Anisotropy Probe (WMAP) Observations: Likelihoods and Parameters from the WMAP data,” *Astrophys. J. Suppl.* **180** (2009) 306–329, arXiv:0803.0586 [astro-ph].
- [48] A. Lewis, A. Challinor, and A. Lasenby, “Efficient Computation of CMB anisotropies in closed FRW models,” *Astrophys. J.* **538** (2000) 473–476, arXiv:astro-ph/9911177.
- [49] M. LoVerde and K. M. Smith, “The Non-Gaussian Halo Mass Function with f_{NL} , g_{NL} and τ_{NL} ,” arXiv:1102.1439 [astro-ph.CO].

- [50] S. Ferraro, M. LoVerde, and K. M. Smith, “Large-scale halo stochasticity and primordial non-Gaussianity,” to appear.
- [51] S. Matarrese, L. Verde, and R. Jimenez, “The abundance of high-redshift objects as a probe of non-Gaussian initial conditions,” *Astrophys. J.* **541** (2000) 10, arXiv:astro-ph/0001366.
- [52] M. LoVerde, A. Miller, S. Shandera, and L. Verde, “Effects of Scale-Dependent Non-Gaussianity on Cosmological Structures,” *JCAP* **0804** (2008) 014, arXiv:0711.4126 [astro-ph].
- [53] S. Chongchitnan and J. Silk, “A Study of High-Order Non-Gaussianity with Applications to Massive Clusters and Large Voids,” *Astrophys. J.* **724** (2010) 285–295, arXiv:1007.1230 [astro-ph.CO].
- [54] T. Y. Lam and R. K. Sheth, “Halo abundances in the f_{nl} model,” arXiv:0905.1702 [astro-ph.CO].
- [55] M. Maggiore and A. Riotto, “The halo mass function from the excursion set method. III. First principle derivation for non-Gaussian theories,” arXiv:0903.1251 [astro-ph.CO].
- [56] A. De Simone, M. Maggiore, and A. Riotto, “Excursion Set Theory for generic moving barriers and non-Gaussian initial conditions,” arXiv:1007.1903 [astro-ph.CO].
- [57] G. D’Amico, M. Musso, J. Norena, and A. Paranjape, “An Improved Calculation of the Non-Gaussian Halo Mass Function,” arXiv:1005.1203 [astro-ph.CO].
- [58] W. H. Press and P. Schechter, “Formation of galaxies and clusters of galaxies by selfsimilar gravitational condensation,” *Astrophys. J.* **187** (1974) 425–438.
- [59] R. K. Sheth and G. Tormen, “Large scale bias and the peak background split,” *Mon. Not. Roy. Astron. Soc.* **308** (1999) 119, arXiv:astro-ph/9901122.
- [60] M. S. Warren, K. Abazajian, D. E. Holz, and L. Teodoro, “Precision Determination of the Mass Function of Dark Matter Halos,” *Astrophys. J.* **646** (2006) 881–885, arXiv:astro-ph/0506395.
- [61] S. Cole and N. Kaiser, “Biased clustering in the cold dark matter cosmogony,” *Mon. Not. Roy. Astron. Soc.* **237** (1989) 1127–1146.
- [62] V. Desjacques and U. Seljak, “Signature of primordial non-Gaussianity of ϕ^3 -type in the mass function and bias of dark matter haloes,” *Phys. Rev.* **D81** (2010) 023006, arXiv:0907.2257 [astro-ph.CO].
- [63] S. Matarrese, F. Lucchin, and S. A. Bonometto, “A Path Integral Approach to Large Scale Matter Distribution Originated by Non-Gaussian Fluctuations,” *Astrophys. J.* **310** (1986) L21–L26.

- [64] V. Springel, “The cosmological simulation code GADGET-2,” *Mon. Not. Roy. Astron. Soc.* **364** (2005) 1105–1134, arXiv:astro-ph/0505010.
- [65] Y. B. Zeldovich, “Gravitational instability: An Approximate theory for large density perturbations,” *Astron. Astrophys.* **5** (1970) 84–89.
- [66] M. Crocce, S. Pueblas, and R. Scoccimarro, “Transients from Initial Conditions in Cosmological Simulations,” *Mon. Not. Roy. Astron. Soc.* **373** (2006) 369–381, arXiv:astro-ph/0606505.
- [67] C. S. Frenk, S. D. M. White, M. Davis, and G. Efstathiou, “The formation of dark halos in a universe dominated by cold dark matter,” *Astrophys. J.* **327** (1988) 507–525.
- [68] K. M. Smith and M. LoVerde, “Local stochastic non-Gaussianity and N-body simulations,” arXiv:1010.0055 [astro-ph.CO].
- [69] B. A. Reid, L. Verde, K. Dolag, S. Matarrese, and L. Moscardini, “Non-Gaussian halo assembly bias,” *JCAP* **1007** (2010) 013, arXiv:1004.1637 [astro-ph.CO].

A Barrier model calculations

In this appendix, we give details of the calculation of the halo mass function and large-scale bias (Eqs. (34)–(40)) in the barrier crossing model, to first order in f_{NL} , g_{NL} .

First, consider evaluation of the integrals in Eqs. (30), (31). Primordial non-Gaussianity enters the calculation by perturbing the PDFs which appear from Gaussian distributions. This perturbation can be written down explicitly using the Edgeworth expansion, which represents the PDF as a power series in cumulants. The Edgeworth expansion for the 1-variable PDF $p(\delta'_M)$ is:

$$\begin{aligned}
p(\delta'_M) &= \exp\left(\sum_{n \geq 3} \frac{(-1)^n}{n!} \kappa_n(M) \sigma_M^n \frac{\partial^n}{\partial \delta'_M{}^n}\right) \frac{1}{(2\pi)^{1/2} \sigma_M} e^{-\delta'^2_M / (2\sigma_M^2)} \\
&= \frac{1}{(2\pi)^{1/2} \sigma_M} e^{-\delta'^2_M / (2\sigma_M^2)} \left(1 + \frac{\kappa_3(M)}{6} H_3(\nu) + \frac{\kappa_4(M)}{24} H_4(\nu) + \dots\right) \\
&= \frac{1}{(2\pi)^{1/2} \sigma_M} e^{-\delta'^2_M / (2\sigma_M^2)} \left(1 + f_{NL} \frac{\kappa_3^{(1)}(M)}{6} H_3(\nu) + g_{NL} \frac{\kappa_4^{(1)}(M)}{24} H_4(\nu) + \dots\right) \quad (52)
\end{aligned}$$

where we have kept terms of first order in f_{NL} , g_{NL} . We can now compute p_0 by plugging into the definition (30):

$$p_0 = \frac{1}{2} \operatorname{erfc}\left(\frac{\nu}{\sqrt{2}}\right) + f_{NL} \frac{\kappa_3^{(1)}(M)}{6} \frac{e^{-\nu^2/2}}{(2\pi)^{1/2}} H_2(\nu) + g_{NL} \frac{\kappa_4^{(1)}(M)}{24} \frac{e^{-\nu^2/2}}{(2\pi)^{1/2}} H_3(\nu) \quad (53)$$

Armed with this expression, it is easy to compute $n(M) = -2\rho_m/M(dp_0/dM)$, obtaining the form of the mass function in Eq. (34).

Moving on to the 2-variable PDF $p(\delta_{\text{lin}}, \delta'_M)$, the Edgeworth expansion is:

$$p(\delta_{\text{lin}}, \delta'_M) = \exp \left(\sigma_{\text{lin}} \sigma_M \kappa_{1,1} \frac{\partial^2}{\partial \delta_{\text{lin}} \partial \delta'_M} + \sum_{\substack{m,n \\ m+n \geq 3}} \frac{(-1)^{m+n}}{m!n!} \sigma_{\text{lin}}^m \sigma_M^n \kappa_{m,n} \frac{\partial^{m+n}}{\partial \delta_{\text{lin}}^m \partial \delta'_M^n} \right) \times \frac{1}{2\pi \sigma_{\text{lin}} \sigma_M} \exp \left(-\frac{\delta_{\text{lin}}^2}{2\sigma_{\text{lin}}^2} - \frac{\delta'_M{}^2}{2\sigma_M^2} \right) \quad (54)$$

where $\sigma_{\text{lin}} = \langle \delta_{\text{lin}}^2 \rangle^{1/2}$ and the cumulant $\kappa_{m,n}$ is defined by:⁹

$$\kappa_{m,n}(M, r) = \frac{\langle (\delta_{\text{lin}})^m (\delta'_M)^n \rangle_{\text{conn}}}{\sigma_{\text{lin}}^m \sigma_M^n} \quad (55)$$

Note that the cumulant $\kappa_n(M)$ defined previously in Eq. (7) is equal to $\kappa_{0,n}(M, r)$.

Keeping the first few terms in the Edgeworth expansion:¹⁰

$$p(\delta_{\text{lin}}, \delta'_M) = \frac{1}{2\pi \sigma_{\text{lin}} \sigma_M} \exp \left(-\frac{\delta_{\text{lin}}^2}{2\sigma_{\text{lin}}^2} - \frac{\delta'_M{}^2}{2\sigma_M^2} \right) \times \left(1 + \frac{\kappa_{1,1}(M, r)}{\sigma_{\text{lin}}} \delta_{\text{lin}} \left(\frac{\delta'_M}{\sigma_M} \right) + \frac{\kappa_{1,2}(M, r)}{2\sigma_{\text{lin}}} \delta_{\text{lin}} H_2 \left(\frac{\delta'_M}{\sigma_M} \right) + \frac{\kappa_{1,3}(M, r)}{6\sigma_{\text{lin}}} \delta_{\text{lin}} H_3 \left(\frac{\delta'_M}{\sigma_M} \right) + \frac{\kappa_{1,1}(M, r) \kappa_{0,3}(M)}{6\sigma_{\text{lin}}} \delta_{\text{lin}} H_4 \left(\frac{\delta'_M}{\sigma_M} \right) + \frac{\kappa_{1,1}(M, r) \kappa_{0,4}(M)}{24\sigma_{\text{lin}}} \delta_{\text{lin}} H_5 \left(\frac{\delta'_M}{\sigma_M} \right) + \dots \right) \quad (56)$$

we compute $\xi_0(r)$ by integrating Eq. (31) term by term, obtaining:

$$\xi_0(r) = \frac{\sigma_{\text{lin}} e^{-\nu^2/2}}{(2\pi)^{1/2}} \left(\kappa_{1,1}(M, r) + \frac{\kappa_{1,2}(M, r)}{2} \nu + \frac{\kappa_{1,3}(M, r)}{6} H_2(\nu) + \frac{\kappa_{1,1}(M, r) \kappa_3(M)}{6} H_3(\nu) + \frac{\kappa_{1,1}(M, r) \kappa_4(M)}{24} H_4(\nu) \right) \quad (57)$$

To make further progress, we convert the correlation function to a power spectrum $P_0(k) = \int d^3 \mathbf{r} e^{i\mathbf{k} \cdot \mathbf{r}} \xi_0(r)$, and keep only the leading behavior of each term in the long-wavelength limit $k \rightarrow 0$.

$$\int d^3 \mathbf{r} e^{i\mathbf{k} \cdot \mathbf{r}} \kappa_{1,2}(M, r) = \frac{1}{\sigma_{\text{lin}} \sigma_M^2} \int \frac{d^3 \mathbf{q} d^3 \mathbf{q}'}{(2\pi)^6} W_M(q) W_M(q') \langle \delta(\mathbf{k}) \delta(\mathbf{q}) \delta(-\mathbf{q}') \rangle \rightarrow \frac{4f_{NL} P(k)}{\sigma_{\text{lin}} \alpha(k)} \quad (58)$$

⁹A technical point: σ_{lin} is formally infinite, but it will cancel from the final results in Eqs. (36)–(40). One could make σ_{lin} finite by introducing a smoothing scale R for the matter field, and take the limit $R \rightarrow 0$ at the end of the calculation.

¹⁰The choice of terms to keep was dictated by the following considerations. Only terms with precisely one δ_{lin} derivative will give nonzero contributions to the integral $\int_{-\infty}^{\infty} d\delta_{\text{lin}} \delta_{\text{lin}} p(\delta_{\text{lin}}, \delta'_M)$ appearing in $\xi_{mh}(r)$, so we have only kept these terms. (Terms with two or more derivatives would contribute to the halo-halo correlation function $\xi_{hh}(r)$, so they may be relevant for halo stochasticity.) We have also omitted terms whose leading contribution is second-order or higher in f_{NL} and g_{NL} .

$$\begin{aligned}
\int d^3\mathbf{r} e^{i\mathbf{k}\cdot\mathbf{r}} \kappa_{1,3}(M, r) &= \frac{1}{\sigma_{\text{lin}}\sigma_M^3} \int \frac{d^3\mathbf{q} d^3\mathbf{q}' d^3\mathbf{q}''}{(2\pi)^9} W_M(q) W_M(q') W_M(q'') \\
&\quad \times \langle \delta(\mathbf{k}) \delta(\mathbf{q}) \delta(\mathbf{q}') \delta(-\mathbf{q}'') \rangle_{\text{conn}} \\
&\rightarrow \frac{18g_{NL}P(k)}{\sigma_{\text{lin}}\sigma_M^3\alpha(k)} \int \frac{d^3\mathbf{q} d^3\mathbf{q}'}{(2\pi)^6} W_M(q) W_M(q') W_M(|\mathbf{q} + \mathbf{q}'|) \\
&\quad \times \frac{P(q)P(q')\alpha(|\mathbf{q} + \mathbf{q}'|)}{\alpha(q)\alpha(q')} \\
&= \frac{3g_{NL}}{\sigma_{\text{lin}}} \kappa_3^{(1)}(M) \left(\frac{P(k)}{\alpha(k)} \right) \tag{59}
\end{aligned}$$

where “ \rightarrow ” denotes the $k \rightarrow 0$ limit, and we have used Eq. (10) to simplify the last line. Putting this together, we find the following expression for $P_0(k)$ in the $k \rightarrow 0$ limit:

$$\begin{aligned}
P_0(k) &= \frac{e^{-\nu^2/2}}{(2\pi)^{1/2}} \left[\frac{P(k)}{\sigma_M} \left(1 + f_{NL} \frac{\kappa_3^{(1)}(M)}{6} H_3(\nu) + g_{NL} \frac{\kappa_4^{(1)}(M)}{24} H_4(\nu) \right) \right. \\
&\quad \left. + 2\nu f_{NL} \frac{P(k)}{\alpha(k)} + \kappa_3^{(1)}(M) \frac{H_2(\nu)}{2} g_{NL} \frac{P(k)}{\alpha(k)} \right] \tag{60}
\end{aligned}$$

The halo bias in a narrow mass range is given by the derivative:

$$b(k) = \frac{dP_0(k)/dM}{(dp_0/dM)P(k)} + 1 \tag{61}$$

where the “+1” converts Lagrangian to Eulerian bias. Plugging in the forms of p_0 , P_0 in Eqs. (53), (60), a long but straightforward calculation now gives the halo bias in the form given in the text (Eqs. (35)–(40)).